Analysis of the dynamical cluster approximation for the Hubbard model

K. Aryanpour,[1] M. H. Hettler,[2] and M. Jarrell[1]
[1]*University of Cincinnati, Cincinnati, Ohio 45221*
[2]*Forschungszentrum Karlsruhe, Institut für Nanotechnologie, Karlsruhe, Germany*
(Received 2 November 2001; published 29 March 2002)

We examine a central approximation of the recently introduced dynamical cluster approximation (DCA) by example of the Hubbard model. By both analytical and numerical means we study noncompact and compact contributions to the thermodynamic potential. We show that approximating noncompact diagrams by their cluster analogs results in a larger systematic error as compared to the compact diagrams. Consequently, only the compact contributions should be taken from the cluster, whereas noncompact graphs should be inferred from the appropriate Dyson equation. The distinction between noncompact and compact diagrams persists even in the limit of infinite dimensions. Nonlocal corrections beyond the DCA exist for the noncompact diagrams, whereas they vanish for compact diagrams.

DOI: 10.1103/PhysRevB.65.153102 PACS number(s): 71.27.+a, 05.10.−a, 05.10.Cc

I. INTRODUCTION

Strongly correlated electron systems are often characterized by short-range dynamical fluctuations. Consequently, local approximations like the dynamical mean-field approximation[1–4] (DMFA) successfully describe many of the qualitative properties. However, in low-dimensional systems, spatial correlations become increasingly important and are thought to be responsible for, e.g., non-Fermi-liquid behavior and *d*-wave pairing in the cuprate superconductors.

The dynamical cluster approximation (DCA) was introduced as a technique to include such nonlocal corrections to the DMFA.[5,6] This is accomplished by mapping the lattice problem onto that of a self-consistently embedded cluster, with periodic boundary conditions.[7] The DCA may also be viewed diagrammatically as an approximation which systematically restores momentum conservation at the internal vertices of many-body Feynman diagrams, which is relinquished in the local DMFA. Here, we investigate one of the central approximations of the DCA: that compact (skeletal) contributions to the thermodynamic potential are well approximated by their cluster counterparts, whereas noncompact (nonskeletal) contributions should not be approximated by their cluster counterparts. Rather, they should be constructed using the appropriate Dyson equation.

II. GENERAL CONSIDERATIONS

Following Baym,[8] a microscopic theory may be defined by its approximation to the generating functional $\Phi[G]$ defining the thermodynamic potential (difference) of the system via

$$\Delta\Omega=\Omega-\Omega_0=-2\,\mathrm{Tr}[\Sigma G-\ln(G/G_0)]+\Phi[G], \quad (1)$$

where G is the full and G_0 the bare one-particle Green function, and Σ the self-energy. $\Phi[G]$ is a sum of all compact (skeletal) closed connected Feynman diagrams. The other contributions to the thermodynamic potential incorporate noncompact diagrams. Typical compact and noncompact diagrams are illustrated in Fig. 1. In the noncompact diagram, two self-energy pieces σ and σ' are connected with two Green functions. In the compact diagram, two vertex parts Γ and Γ' are connected with four Green functions.[7]

As shown by Müller-Hartmann,[2] the DMFA may be defined by relinquishing the momentum conservation at each internal vertex in $\Phi[G]$.[9] This conservation is described by the Laue function

$$\Delta=\sum_{\mathbf{x}} e^{i\mathbf{x}\cdot(\mathbf{k}_1+\mathbf{k}_2-\mathbf{k}_3-\mathbf{k}_4)}=N\delta_{\mathbf{k}_1+\mathbf{k}_2,\mathbf{k}_3+\mathbf{k}_4}. \quad (2)$$

In the DMFA, momentum conservation is completely abandoned and the Laue function $\Delta_{DMFA}\equiv 1$. We may then sum freely over all the internal momenta labels.

The DCA is constructed to systematically restore the momentum conservation at each internal vertex by mapping the lattice onto a self-consistently embedded cluster problem. We have provided a microscopic definition of the DCA through its Laue function. However, to clarify the relation between this microscopic definition and the cluster problem, we must first decompose the lattice into clusters and define the corresponding problem in reciprocal space. Here, the real lattice of N sites is tiled by N/N_c clusters, each composed of $N_c=L^D$ sites where D is dimensionality and L the size of clusters (cf. Fig. 2 for $L=D=2$). We label the origin of the clusters by $\tilde{\mathbf{x}}$ and the N_c intracluster sites by $\mathbf{X}$. So for each site in the original lattice $\mathbf{x}=\mathbf{X}+\tilde{\mathbf{x}}$. In reciprocal space, the points $\tilde{\mathbf{x}}$ and $\mathbf{X}$ form lattices labeled by $\tilde{\mathbf{k}}$ and $\mathbf{K}$, respectively, with $K_\alpha=n_\alpha 2\pi/L$ and integer n_α. Then $\mathbf{k}=\mathbf{K}+\tilde{\mathbf{k}}$ (see Fig. 2).

In the DCA, we first make the separation

$$\Delta=\frac{N}{N_c}\delta_{\tilde{\mathbf{k}}_1+\tilde{\mathbf{k}}_2,\tilde{\mathbf{k}}_3+\tilde{\mathbf{k}}_4}N_c\delta_{\mathbf{K}_1+\mathbf{K}_2,\mathbf{K}_3+\mathbf{K}_4} \quad (3)$$

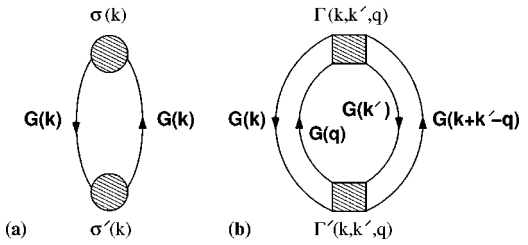

FIG. 1. (a) Typical noncompact (nonskeletal) and (b) typical compact (skeletal) diagrams.

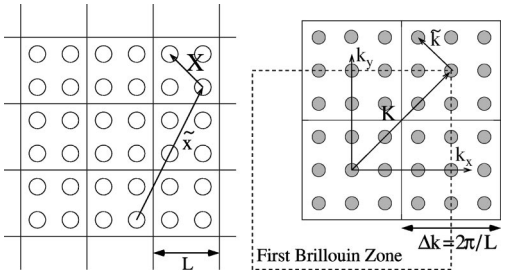

FIG. 2. The real lattice cluster (left) and the first Brillouin zone (right) divided into subcells.

and then set $N/N_c\delta_{\tilde{\mathbf{k}}_1+\tilde{\mathbf{k}}_2,\tilde{\mathbf{k}}_3+\tilde{\mathbf{k}}_4}\cong 1$, so that

$$\Delta_{DCA}=N_c\delta_{\mathbf{K}_1+\mathbf{K}_2,\mathbf{K}_3+\mathbf{K}_4}, \tag{4}$$

which indicates that the momentum is partially conserved for transfers between the cells.

In this paper, we consider the approximation made through the substitution $\Delta\rightarrow\Delta_{DCA}$ in the compact and noncompact contributions to the thermodynamic potential. Whenever the substitution is made, all internal legs are replaced by the coarse grained Green function defined by

$$\overline{G}(\mathbf{K},z)=\frac{N_c}{N}\sum_{\tilde{\mathbf{k}}} G(\mathbf{K}+\tilde{\mathbf{k}},z). \tag{5}$$

The corresponding estimate of the self-energy will then necessarily be a function of $\mathbf{K}$ and (complex) frequency z. The DCA estimate of the lattice Green function is then given by

$$G(\mathbf{k},z)=\frac{1}{z-\epsilon_{\mathbf{k}}+\mu-\Sigma_{DCA}(\mathbf{K},z)}. \tag{6}$$

It is of importance to note that by using Eq. (6) we have already made the approximation $\Sigma(k,z)=\Sigma_{DCA}(\mathbf{K},z)+\mathcal{O}((\Delta ka)^2)$ where Δk is the size of the coarse graining cell shown in Fig. 2 and a is the lattice constant (chosen as unity). We also drop the frequency label from this point on for simplicity.

III. COARSE GRAINING COMPACT VS. NON-COMPACT DIAGRAMS

We investigate the additional approximations associated with coarse graining in compact and noncompact diagrams. To do this we will consider diagrams with all legs coarse grained, except those explicitly displayed in Figs. 3 and 4. Consider the first nontrivial correction to the coarse-grained noncompact diagrams as illustrated in Fig. 3:

$$\begin{aligned}\delta^{(1)}[\Delta\Omega_{ncp}]\sim&\frac{1}{N_c}\sum_{\mathbf{K}_1,\mathbf{K}_2}\sigma(\mathbf{K}_1,\mathbf{K}_2)\sigma'(\mathbf{K}_1,\mathbf{K}_2)\\&\times\int_{-\infty}^{\infty}\int_{-\infty}^{\infty}d\epsilon_1 d\epsilon_2 G(\mathbf{K}_1,\epsilon_1)G(\mathbf{K}_2,\epsilon_2)\\&\times[\rho_{ncp}(\epsilon_1,\mathbf{K}_1;\epsilon_2,\mathbf{K}_2)\\&-\overline{\rho}_{ncp}(\epsilon_1,\mathbf{K}_1;\epsilon_2,\mathbf{K}_2)]\delta_{\mathbf{K}_2,\mathbf{K}_1},\end{aligned} \tag{7}$$

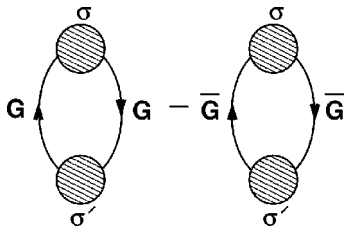

FIG. 3. First correction by noncompact diagrams, $\delta^{(1)}[\Delta\Omega_{ncp}]$.

where

$$\begin{aligned}\rho_{ncp}(\epsilon_1,\mathbf{K}_1;\epsilon_2,\mathbf{K}_2)=&\frac{N_c}{N}\sum_{\tilde{\mathbf{k}}_1,\tilde{\mathbf{k}}_2}\delta(\epsilon_1-\epsilon_{\mathbf{K}_1+\tilde{\mathbf{k}}_1})\\&\times\delta(\epsilon_2-\epsilon_{\mathbf{K}_2+\tilde{\mathbf{k}}_2})\delta_{\tilde{\mathbf{k}}_2,\tilde{\mathbf{k}}_1}\end{aligned} \tag{8}$$

and

$$\begin{aligned}&\overline{\rho}_{ncp}(\epsilon_1,\mathbf{K}_1;\epsilon_2,\mathbf{K}_2)\\&\quad=\frac{N_c^2}{N^2}\sum_{\tilde{\mathbf{k}}_1,\tilde{\mathbf{k}}_2}\delta(\epsilon_1-\epsilon_{\mathbf{K}_1+\tilde{\mathbf{k}}_1})\delta(\epsilon_2-\epsilon_{\mathbf{K}_2+\tilde{\mathbf{k}}_2}).\end{aligned} \tag{9}$$

In the above derivations we assumed that the self-energy is $\tilde{\mathbf{k}}$ independent and therefore the entire $\tilde{\mathbf{k}}$ dependence of the Green function is only through the dispersion ϵ given by

$$\epsilon_{\mathbf{K}+\tilde{\mathbf{k}}}=-2t/(2D)^{1/2}\sum_{n=1}^{D}\cos(\mathbf{K}_n+\tilde{\mathbf{k}}_n), \tag{10}$$

which is just the noninteracting dispersion of the Hubbard model Hamiltonian with nearest-neighbor hoppings and dimensionality D. By the same token, in Fig. 4, for the compact part with coarse-grained Γ and Γ' we have

$$\begin{aligned}\delta^{(1)}[\Delta\Omega_{cp}]\sim&\frac{1}{N_c^3}\sum_{\substack{\mathbf{K}_1,\mathbf{K}_2\\\mathbf{K}_3,\mathbf{K}_4}}\delta_{\mathbf{K}_4,\mathbf{K}_1+\mathbf{K}_2-\mathbf{K}_3}\Gamma(\mathbf{K}_1,\mathbf{K}_2,\mathbf{K}_3,\mathbf{K}_4)\\&\times\Gamma'(\mathbf{K}_1,\mathbf{K}_2,\mathbf{K}_3,\mathbf{K}_4)\\&\times\int_{-\infty}^{\infty}\int_{-\infty}^{\infty}\int_{-\infty}^{\infty}\int_{-\infty}^{\infty}d\epsilon_1 d\epsilon_2 d\epsilon_3 d\epsilon_4\\&\times G(\mathbf{K}_1,\epsilon_1)G(\mathbf{K}_2,\epsilon_2)G(\mathbf{K}_3,\epsilon_3)G(\mathbf{K}_4,\epsilon_4)\\&\times[\rho_{cp}(\epsilon_1,\mathbf{K}_1;\epsilon_2,\mathbf{K}_2;\epsilon_3,\mathbf{K}_3;\epsilon_4,\mathbf{K}_4)\\&-\overline{\rho}_{cp}(\epsilon_1,\mathbf{K}_1;\epsilon_2,\mathbf{K}_2;\epsilon_3,\mathbf{K}_3;\epsilon_4,\mathbf{K}_4)],\end{aligned} \tag{11}$$

where

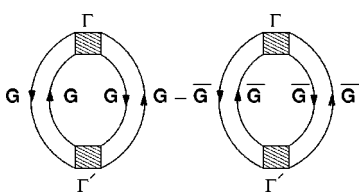

FIG. 4. First correction by compact diagrams, $\delta^{(1)}[\Delta\Omega_{cp}]$.

$$\rho_{cp}(\epsilon_1,\mathbf{K}_1;\epsilon_2,\mathbf{K}_2;\epsilon_3,\mathbf{K}_3;\epsilon_4,\mathbf{K}_4) = \frac{N_c^3}{N^3}\sum_{\substack{\tilde{\mathbf{k}}_1,\tilde{\mathbf{k}}_2\\ \tilde{\mathbf{k}}_3,\tilde{\mathbf{k}}_4}} \delta(\epsilon_1-\epsilon_{\mathbf{K}_1+\tilde{\mathbf{k}}_1})\,\delta(\epsilon_2-\epsilon_{\mathbf{K}_2+\tilde{\mathbf{k}}_2}) \times \delta(\epsilon_3-\epsilon_{\mathbf{K}_3+\tilde{\mathbf{k}}_3})\,\delta(\epsilon_4-\epsilon_{\mathbf{K}_4+\tilde{\mathbf{k}}_4})\,\delta_{\tilde{\mathbf{k}}_4,\tilde{\mathbf{k}}_1+\tilde{\mathbf{k}}_2-\tilde{\mathbf{k}}_3} \quad (12)$$

and

$$\overline{\rho}_{cp}(\epsilon_1,\mathbf{K}_1;\epsilon_2,\mathbf{K}_2;\epsilon_3,\mathbf{K}_3;\epsilon_4,\mathbf{K}_4) = \frac{N_c^4}{N^4}\sum_{\substack{\tilde{\mathbf{k}}_1,\tilde{\mathbf{k}}_2\\ \tilde{\mathbf{k}}_3,\tilde{\mathbf{k}}_4}} \delta(\epsilon_1-\epsilon_{\mathbf{K}_1+\tilde{\mathbf{k}}_1})\,\delta(\epsilon_2-\epsilon_{\mathbf{K}_2+\tilde{\mathbf{k}}_2}) \times \delta(\epsilon_3-\epsilon_{\mathbf{K}_3+\tilde{\mathbf{k}}_3})\,\delta(\epsilon_4-\epsilon_{\mathbf{K}_4+\tilde{\mathbf{k}}_4}). \quad (13)$$

We now define the Fourier transforms of ρ and $\overline{\rho}$ with respect to the energy arguments, e.g.,

$$\Psi(s,\mathbf{K}) = \int_{-\infty}^{\infty} \rho(\epsilon,\mathbf{K}) e^{is\epsilon} d\epsilon. \quad (14)$$

For the noncompact corrections, Eq. (14) defines $\Psi_{ncp}(s_1,\mathbf{K}_1;s_2,\mathbf{K}_2)$ and $\overline{\Psi}_{ncp}(s_1,\mathbf{K}_1;s_2,\mathbf{K}_2)$, respectively. In order to calculate the difference between Ψ and $\overline{\Psi}$ in finite dimensions, we expand the dispersions and exponentials as functions of $\tilde{\mathbf{k}}$ and keep the terms up to Δk^2. The difference $\delta\Psi_{ncp}$ for the noncompact diagrams becomes

$$\delta\Psi_{ncp}(s_1,\mathbf{K}_1;s_2,\mathbf{K}_2) \approx \frac{t^2}{3}\Delta k^2[\,\eta(\mathbf{K}_1+\mathbf{K}_2) - \eta(\mathbf{K}_1-\mathbf{K}_2)]s_1 s_2 \exp[i(s_1\epsilon_{\mathbf{K}_1}+s_2\epsilon_{\mathbf{K}_2})], \quad (15)$$

where $\eta(\mathbf{K}) = 1/D\,\Sigma_n \cos(\mathbf{K}_n)$. Reversing the Fourier transform then yields for the difference of ρ_{ncp} and $\overline{\rho}_{ncp}$

$$\delta\rho_{ncp}(\epsilon_1,\mathbf{K}_1;\epsilon_2,\mathbf{K}_2) \approx -\frac{t^2}{3}\Delta k^2[\,\eta(\mathbf{K}_1+\mathbf{K}_2) - \eta(\mathbf{K}_1-\mathbf{K}_2)]\frac{\partial}{\partial\epsilon_1}\delta(\epsilon_1-\epsilon_{\mathbf{K}_1})\frac{\partial}{\partial\epsilon_2}\delta(\epsilon_2-\epsilon_{\mathbf{K}_2}). \quad (16)$$

Equation (16) demonstrates that the difference between coarse graining and no coarse graining in noncompact diagrams yields an error of order Δk^2. After a tedious but straightforward calculation for the corresponding difference between coarse graining and no coarse graining in compact diagrams we obtain $\delta\rho_{cp}\sim\mathcal{O}(\Delta k^6)$. Since $\Delta k = 2\pi/L$, for large clusters this error becomes much smaller than the error in Eq. (16).

To illustrate the above point we simulate a two–dimensional Hubbard model (with local interaction U and a nearest-neighbor hopping $t=1$) using the fluctuation exchange approximation (FLEX).[10] We employ an elaborate subtraction scheme to correctly deal with the high-frequency behavior of the Green functions and FLEX potentials.[11] In Figs. 5 and 6 the compact and noncompact parts of $\Delta\Omega$ have been plotted for the interaction $U=1.57$ for various cluster sizes L and temperatures T. In Fig. 5, it is readily seen that for the compact contribution with coarse-grained Green functions the variation of Ω_{cp} over the entire Δk range is roughly 10%. In contrast, as shown in Fig. 6, the difference between the noncompact contributions with and without coarse graining generates deviations of over 100%. Note that at very low temperatures (inset in Fig. 5) the deviation from linearity for $T<0.066$ is due to the correlation length exceeding the size of cluster L. Then, the DCA assumption of replacing $\Sigma(\mathbf{k})$ by $\Sigma_{DCA}(\mathbf{K})$ is no longer valid.

IV. LIMIT OF INFINITE DIMENSIONS

To make contact with the original derivations of the DMFA,[1,2] we explore the differences between the compact and noncompact graphs in the limit of many spatial dimen-

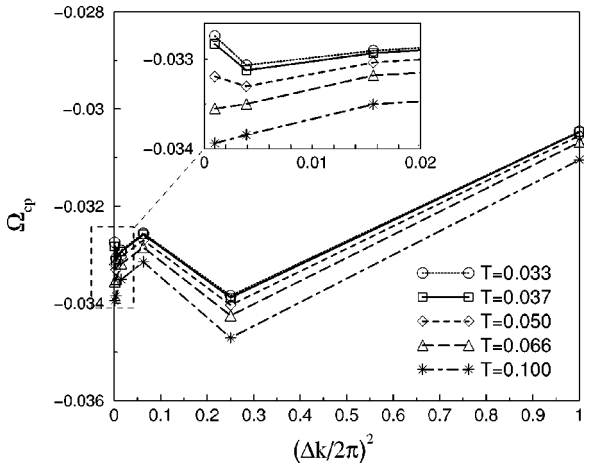

FIG. 5. The compact contribution of the thermodynamic potential vs Δk^2 using the FLEX method for $U=1.57$.

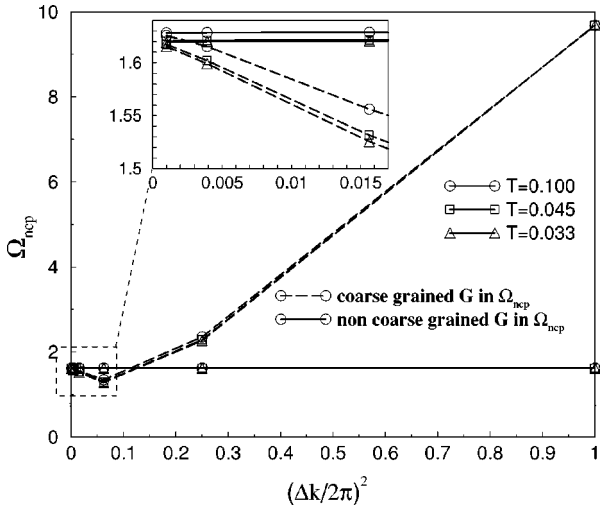

FIG. 6. Noncompact contributions of the thermodynamic potential with and without coarse graining for $U=1.57$.

sions D. For $D\rightarrow\infty$, we calculate $\Delta\rho$ for both compact and noncompact diagrams by simply expanding Ψ and $\overline{\Psi}$ but this time with respect to $1/D$ instead of Δk^2. Letting $D\rightarrow\infty$ we can show that

$$\lim_{D\rightarrow\infty}\Psi_{ncp}(s_1,\mathbf{K}_1;s_2,\mathbf{K}_2)$$
$$\approx\overline{\Psi}_{D\rightarrow\infty}\times\exp\left(\frac{-t^2}{12}\Delta k^2[\,\eta(\mathbf{K}_2-\mathbf{K}_1)-\eta(\mathbf{K}_1+\mathbf{K}_2)]s_1s_2\right). \quad (17)$$

Expanding the exponential in Eq. (17),

$$\lim_{D\rightarrow\infty}\Psi_{ncp}(s_1,\mathbf{K}_1;s_2,\mathbf{K}_2)$$
$$\approx\overline{\Psi}_{D\rightarrow\infty}\times\left(1-\frac{t^2}{12}\Delta k^2[\,\eta(\mathbf{K}_2-\mathbf{K}_1)-\eta(\mathbf{K}_1+\mathbf{K}_2)]s_1s_2+\cdots\right) \quad (18)$$

and, consequently,

$$\lim_{D\rightarrow\infty}\delta\rho_{ncp}(\epsilon_1,\mathbf{K}_1;\epsilon_2,\mathbf{K}_2)$$
$$\approx\frac{t^2}{12}\Delta k^2[\,\eta(\mathbf{K}_2-\mathbf{K}_1)-\eta(\mathbf{K}_1+\mathbf{K}_2)]$$
$$\times\frac{\partial}{\partial\epsilon_1}\frac{\partial}{\partial\epsilon_2}\overline{\rho}_{D\rightarrow\infty}(\epsilon_1,\mathbf{K}_1;\epsilon_2,\mathbf{K}_2)+\mathcal{O}(\Delta k^4). \quad (19)$$

However, for the difference in the compact diagrams as $D\rightarrow\infty$ we find $\lim_{D\rightarrow\infty}\delta\Psi_{cp}=0$. Thus, for all Δk, there are nonlocal corrections to noncompact diagrams while there are none to compact diagrams as $D\rightarrow\infty$. This result is consistent with what Müller-Hartmann has shown for the DMFA.[2] Regardless of whether the expansion parameter is Δk or $1/D$, there is a fundamental difference between compact and noncompact diagrams which requires different treatments of each. Consequently, only the compact contributions should be formed from coarse-grained Green functions, whereas noncompact graphs should be inferred from the appropriate Dyson equation.

Finally, even though we directly invoked the nearest-neighbor hopping dispersion in our algorithm, our arguments can be generalized to other models assuming that the Green function falls off exponentially as $G(r)\sim e^{-r/r_s}$ where r_s is a characteristic length depending on dimensionality. It turns out that the compact diagrams fall off much faster due to having a larger number of Green functions relative to the noncompact ones which again explains why we coarse grain the Green functions in only the compact part of the free energy difference. The arguments made here may also be applied to the DMFA simply by taking $N_c=1$. They also may be extended to other cluster approaches, such as the molecular coherent potential approximation[12] and its formal equivalent for dynamical systems the molecular cluster dynamical mean field.[13]

V. CONCLUSIONS

We justify one of the central underlying approximations of the dynamical cluster approximation. We both analytically and numerically demonstrate that coarse graining the Green functions in noncompact diagrams results in a larger amount of error compared to that incurred in compact diagrams. Consequently, noncompact diagrams and their contribution to the thermodynamic potential are not coarse grained. The distinction between noncompact and compact diagrams persists even in the limit of infinite dimensions. This concurs with previous work on dynamical mean-field theory and has implications for other cluster approaches.

We would like to acknowledge Th. Maier, R. Jamei, and A. Voigt for very useful discussions. This work was supported by NSF Grant No. DMR-0073308.

[1] W. Metzner and D. Vollhardt, Phys. Rev. Lett. **62**, 324 (1989).
[2] E. Müller-Hartmann, Z. Phys. B: Condens. Matter **74**, 507 (1989).
[3] T. Pruschke, M. Jarrell, and J.K. Freericks, Adv. Phys. **42**, 187 (1995).
[4] A. Georges *et al.*, Rev. Mod. Phys. **68**, 13 (1996).
[5] M.H. Hettler *et al.*, Phys. Rev. B **58**, 7475 (1998).
[6] M.H. Hettler *et al.*, Phys. Rev. B **61**, 12 739 (2000).
[7] A.A. Abrikosov, L.P. Gorkov, and I.E. Dzyaloshinski, *Methods of Quantum Field Theory in Statistical Physics* (Dover, New York, 1975).
[8] G. Baym, Phys. Rev. **127**, 1391 (1962).
[9] Müller-Hartmann (Ref. 2) actually showed this for self-energy diagrams.
[10] N.E. Bickers *et al.*, Phys. Rev. B **43**, 8044 (1990).
[11] J.J. Deisz *et al.*, in *Recent Progress In Many Body Theories*, edited by E. Schachinger *et al.* (Plenum, New York, 2001), Vol. 4.
[12] F. Ducastelle, J. Phys. C **7**, 1795 (1974).
[13] G. Kotliar, S.Y. Savrasov, and G. Palsson, Phys. Rev. Lett. **87**, 186401 (2001).